Neurochemical and Ultrastructural Characterization of Unmyelinated Non-peptidergic C-Nociceptors and C-Low Threshold Mechanoreceptors Projecting to Lamina II of the Mouse Spinal Cord

Chiara Salio, Patrizia Aimar, Pascale Malapert, Aziz Moqrich, Adalberto Merighi

Cellular and Molecular Neurobiology
https://doi.org/10.1007/s10571-020-00847-w

ORIGINAL RESEARCH

Neurochemical and Ultrastructural Characterization of Unmyelinated Non-peptidergic C-Nociceptors and C-Low Threshold Mechanoreceptors Projecting to Lamina II of the Mouse Spinal Cord

Chiara Salio[1] · Patrizia Aimar[1] · Pascale Malapert[2] · Aziz Moqrich[2] · Adalberto Merighi[1]

Received: 14 February 2020 / Accepted: 9 April 2020

Abstract

C-nociceptors (C-Ncs) and non-nociceptive C-low threshold mechanoreceptors (C-LTMRs) are two subpopulations of small unmyelinated non-peptidergic C-type neurons of the dorsal root ganglia (DRGs) with central projections displaying a specific pattern of termination in the spinal cord dorsal horn. Although these two subpopulations exist in several animals, remarkable neurochemical differences occur between mammals, particularly rat/humans from one side and mouse from the other. Mouse is widely investigated by transcriptomics. Therefore, we here studied the immunocytochemistry of murine C-type DRG neurons and their central terminals in spinal lamina II at light and electron microscopic levels. We used a panel of markers for peptidergic (CGRP), non-peptidergic (IB4), nociceptive (TRPV1), non-nociceptive (VGLUT3) C-type neurons and two strains of transgenic mice: the TAFA4^{Venus} knock-in mouse to localize the TAFA4^{+} C-LTMRs, and a genetically engineered *ginip* mouse that allows an inducible and tissue-specific ablation of the DRG neurons expressing GINIP, a key modulator of $GABA_BR$-mediated analgesia. We confirmed that IB4 and TAFA4 did not coexist in small non-peptidergic C-type DRG neurons and separately tagged the C-Ncs and the C-LTMRs. We then showed that TRPV1 was expressed in only about 7% of the IB4^{+} non-peptidergic C-Ncs and their type Ia glomerular terminals within lamina II. Notably, the selective ablation of GINIP did not affect these neurons, whereas it reduced IB4 labeling in the medial part of lamina II and the density of C-LTMRs glomerular terminals to about one half throughout the entire lamina. We discuss the significance of these findings for interspecies differences and functional relevance.

Keywords Non-peptidergic C-Ncs · C-LTMRs · IB4 · TAFA4 · GINIP · TRPV1

Introduction

Lamina II of the spinal gray matter not only modulates nociception at the synaptic interface between first-order sensory neurons in the dorsal root ganglia (DRGs) and second-order projection neurons in laminae I and III–V of the dorsal horn, but is also implicated in the integration of non-nociceptive mechanical and thermal stimuli, pleasant touch and itch (Merighi 2018).

✉ Adalberto Merighi
adalberto.merighi@unito.it

[1] Department of Veterinary Sciences, University of Turin, 10095 Grugliasco, Italy

[2] Aix-Marseille-Université, CNRS, Institut de Biologie du Développement de Marseille, UMR 7288, case 907, 13288 Marseille Cedex 09, France

DRG neurons are of heterogeneous sizes and the smallest ones (type C neurons), which in rodents are 20 µm or less in diameter, give rise to small diameter unmyelinated somatic or visceral C-type primary afferent fibers, herein simply indicated as C-fibers, which were initially demonstrated to have a slow conductance and high thresholds of activation (Lawson et al. 1993). Therefore, until recently, it was believed that the type C DRG neurons, and hence their C-fibers, were only activated by noxious stimuli, albeit of heterogeneous nature (mechanical, thermal, chemical), and were commonly referred to as C-type nociceptors (C-Ncs).

In rodents, current classification of C-Ncs postulates the existence of two main populations of peptidergic and non-peptidergic neurons, based on histological, neurochemical and physiological properties; morphology of peripheral projections; and pattern of central termination into the spinal cord dorsal horn. The most accepted view was that the C-type non-peptidergic DRG nociceptive neurons projected

Published online: 18 April 2020

to the inner part of lamina II (II_i) (Silverman and Kruger 1990), and at least in mouse, formed a neurochemically homogenous population labeled by the isolectin B4 from *Griffonia simplicifolia* (IB4) (Strictly speaking, IB4 binds to some sugar residues that are present at the cellular membrane of positive neurons. For the sake of simplicity, these neurons will be indicated as $IB4^+$ to differentiate them from the $IB4^-$ neurons that are unable to bind the lectin) and/or the LA4 antibody (Stucky and Lewin 1999; Braz et al. 2005; Cavanaugh et al. 2009), whereas in rat there was not a neat distinction between peptidergic and non-peptidergic C-Ncs in relation to IB4 binding (Price and Flores 2007). However, in the more recent past, it became clear that these neurons, at least in mouse, also encompassed a subpopulation that did not respond to noxious stimuli. Such a change of opinion largely derived from the continuous discovery of novel neurochemical and functional markers (Le Pichon and Chesler 2014), and from the application of single-cell transcriptomics to cluster murine DRG neurons into more specific functional subpopulations (Usoskin et al. 2015; Zheng et al. 2019).

Thus, it is today accepted that some C-type non-peptidergic DRG neurons are not nociceptors, but, instead, low-threshold mechanoreceptors (C-LTMRs), with slow conduction velocity, low thresholds of activation (Abraira and Ginty 2013; Pitcher et al. 2016) and specific projections to the ventral part of inner lamina II (II_{iv}) of the spinal cord (Li et al. 2011). In parallel, it was demonstrated that these non-peptidergic C-LTMRs contribute to gentle touch under normal conditions (Olausson et al. 2002; Seal et al. 2009; Vrontou et al. 2013) and touch hypersensitivity after injury (Seal et al. 2009; Delfini et al. 2013). Their neurochemistry was, at first, characterized by expression of the vesicular glutamate transporter type 3 (VGLUT3) (Seal et al. 2009), but, later, two other markers joined in the chemokine-like secreted protein TAFA4 and the Gαi-interacting protein GINIP. These two proteins were not mere additional markers, as they acted as new C-LTMR modulators to be activated only in certain injury-mediated general pain conditions, such was the case of TAFA4 (Delfini et al. 2013; Kambrun et al. 2018), or mechanical neuropathic pain, for GINIP (Gaillard et al. 2014; Liu et al. 2016). However, GINIP was expressed not only in $VGLUT3^+/TAFA4^+$ non-peptidergic C-LTMRs, but also in $IB4^+$ non-peptidergic C-Ncs (Reynders et al. 2015; Urien et al. 2017). This latter observation was in some way confusing and rendered even more difficult to frame the organization of the non-peptidergic DRG neurons and their C-fibers into a coherent picture. It remains, in fact, quite difficult to substantiate the idea that the two subpopulations of C-Ncs and C-LTMRs are, indeed, fully distinguishable in neurochemical and functional terms. Further complexity was after that added because 30% of the peptidergic neurons that were immunoreactive for the calcitonin gene-related peptide (CGRP) and the transient receptor potential vanilloid 1 (TRPV1) also contained GINIP, at least in rat (Liu et al. 2016). This observation was puzzling for several reasons. First, CGRP is a well-recognized general peptidergic marker of the DRG neurons throughout species (Gibson et al. 1984) but, at the minimum in rat, it is considered to label the nociceptors irrespectively that they give rise to C or Aδ fibers (Lawson et al. 1996). Second, TRPV1 is a transduction molecule that is also specifically expressed in nociceptors (Patil et al. 2018) but has a quite variegated and controversial tissue distribution across species. To be precise, in rats both peptidergic and non-peptidergic C-Ncs expressed TRPV1 (Tominaga et al. 1998; Guo et al. 1999; Michael and Priestley 1999; Woodbury et al. 2004; Hwang et al. 2005), and in a similar fashion, TRPV1 was detected in larger proportion of human DRG nociceptors compared to mice (Haberberger et al. 2019). However, in mouse C-Ncs, irrespectively of their neuropeptide content, expressed TRPV1 during development, but the receptor became limited to the peptidergic subpopulation in adulthood (Cavanaugh et al. 2011). Nonetheless, according to some authors 2–4.5% of the non-peptidergic $IB4^+$ C-Ncs also expressed TRPV1 (Zwick et al. 2002; Woodbury et al. 2004; Breese et al. 2005) and their number increased during inflammation (Breese et al. 2005).

Thus, several questions still need answering to classify properly the non-peptidergic C-type DRG neurons in mouse as it is not clear yet if, under normal conditions, *all* C-LTMRs are non-nociceptive, and what is the functional importance of GINIP in these neurons.

To provide some answers to these questions and better characterize the different subpopulations of mouse non-peptidergic C-type DRG neurons and their fibers, we have here investigated two different strains of transgenic animals. The first was a $TAFA4^{Venus}$ knock-in mouse expressing the green fluorescent protein (GFP) variant *Venus* in a population of $TAFA4^+$ non-peptidergic C-LTMRs (Delfini et al. 2013). The second was a genetically engineered *ginip* mouse that allows an inducible and tissue-specific ablation of GINIP-expressing sensory neurons in DRGs (Urien et al. 2017).

Experimental Procedures

Animals

Young adult (2–3 months) male mice were housed in a temperature-controlled room (22 °C, 40% humidity), under a 12-h light–dark cycles, and with free access to food and water. The number of the animals used in this study was reduced as much as possible and all efforts were employed to minimize their stress and suffering during all experimental procedures. Work was performed on male mice only to save transgenic females for breeding that was

carried out with harem mating (≥ 3 females/male) on estimates made according to the National Research Council (US) Committee on Guidelines for the Use of Animals in Neuroscience and Behavioral Research (2003). Yet, recent findings indicate that there are no sex differences after RNA-seq transcriptomic experiments in mouse DRGs, both in basal and experimental neuropathic conditions (Lopes et al. 2017). Similarly, a study in rat, which was also focused on the occurrence of sex differences in gene regulation in DRGs after nerve injury (Stephens et al. 2019), found that, after analysis of the expression levels of 14,403 genes in naïve male and females, there were no significant differences in 94.0% of cases. Notably, the list of the 862 genes with expression amounts that differed significantly between the two sexes did not include those encoding for CGRP, VGLUT3, GINIP, TAFA4 or TRPV1. Therefore, we are confident that the results of our present work can be generalized to animals of both sexes.

All experiments were conducted in conformity with the directive (2010/63/EU) of the European Parliament and of the Council of September 22, 2010, with an authorization for animal experimentation by the Italian Ministry of Health (600.8/82.20/AG1826), the French Ministry of Agriculture and the European Community Council Directive (2015070217242262-V5#1537). The animals used in the study were:

(1) Sixteen TAFA4^{Venus} heterozygous $^{(\pm)}$ knock in mice (Delfini et al. 2013) [$n = 8$ for light microscopy (LM) immunofluorescence (IMF) studies divided in $n = 3$ for DRGs and $n = 5$ for spinal cord; $n = 8$ for electron microscopy (EM) studies, divided in $n = 4$ for post-embedding staining procedures and $n = 4$ for pre-embedding Fluoronanogold staining]. We have used these mice to localize the TAFA4-expressing neurons in DRGs and spinal cord. They specifically express the GFP variant *Venus* in TAFA4^{+} C-LTMRs. Thus, for the sake of simplicity, we will indicate GFP expressing neurons as TAFA4^{+} in both text and figures.
(2) Twelve 3-week-old GINIP mice received two intraperitoneal injections of diphtheria toxin (DT; 20 µg/kg), separated by 72-h interval ($n = 3$ controls and $n = 3$ DT for LM; $n = 3$ control and $n = 3$ DT for EM). Spinal cord tissues were prepared 5 weeks after DT injections following the same method reported in two previous publications (Salio et al. 2005; Calorio et al. 2019).
(3) Six CD1 mice ($n = 3$ for LM; $n = 3$ for EM), as control animals to verify peptidergic and non-peptidergic marker expression in genetically unmodified animals.

We sampled the DRGs and the spinal cord after deep pentobarbital anesthesia (3 mg/100 g body weight, intraperitoneal) following standard procedures (see Salio et al. 2005).

LM

Anesthetized animals were perfused with Ringer's solution followed by 4% paraformaldehyde in 0.1 M phosphate buffer (PB). The L1–L6 lumbar spinal cord segments and the corresponding DRGs were dissected out and post-fixed for two additional h in the same fixative. Spinal cord segments were cut with a vibratome (70 µm); DRGs were cryoprotected by overnight incubation in 30% sucrose and then cut at 10 µm with a cryostat. Alternatively, DRGs were dehydrated and embedded in paraffin wax and eventually cut at 10 µm with a microtome.

Multiple IMF

Free-floating vibratome spinal cord sections (from CD1, TAFA4^{Venus} and GINIP-mice) and DRG sections (from CD1 and TAFA4^{Venus} mice) were processed following the standard procedures (Table 1 and Salio et al. 2005).

Previous and the present studies, as referenced in Table 1, provided full validation of all primary antibodies. Specificity controls consisted in omission of primary antibodies and/or pre-absorption tests with the corresponding immunogenic peptides. Method controls consisted in omission of secondary antibodies and/or their substitution with species inappropriate reagent.

The paraformaldehyde vapor blocking method, originally proposed by Wang and Larsson (1985), was used for VGLUT3+TRPV1, VGLUT3+CGRP and CGRP+TRPV1 double IMF experiments, because the two primary antibodies were raised in the same species (Salio et al. 2005).

For the experiments with GINIP mice, sections from control and DT-treated animals were processed together by an operator unaware of the experimental group.

Single-channel stack images from spinal cord sections and single-channel snapshot images from DRGs sections at 20 × were acquired using a Leica TCS SP5 confocal laser scanning microscope (Leica Microsystems, Wetzlar, Germany) with appropriate filter settings and merged using Photoshop CS2 9 (Adobe Systems, San Jose, CA, USA).

EM

Anesthetized animals were perfused with Ringer's solution followed by 4% paraformaldehyde + 0.1% glutaraldehyde. The spinal cord was processed for EM studies as indicated in Table 2. Immunostained sections were observed with a JEM-1010 transmission electron microscope (Jeol, Tokyo, Japan) equipped with a side-mounted CCD camera (Mega View III, Olympus Soft Imaging System, Brandeburg, Germany).

Table 1 Antibodies and buffer solutions for immunofluorescence

Primary antibodies or biotin-conjugate	References for antibody specificity	LM Pre-incubation buffer	LM Secondary antibodies
Rabbit anti-VGLUT3 (1:200) Abcam ab23977	*	PBS–5% NGS	Anti-rabbit Alexa Fluor 488/633 (1:500) Life Technologies
Chicken anti-GFP (1:200) Aves Labs GFP-1020	Kambrun et al. (2018)	PBS–5% NGS	Anti-chicken Alexa Fluor 488 (1:500) Life Technologies
Rabbit anti-TRPV1 (1:1000) Alomone ACC-030	*	PBS–5% NGS	Anti-rabbit Alexa Fluor 594/633 (1:500) Life Technologies
Rat anti-GINIP (1:100) Gaillard et al. (2014)	Gaillard et al. (2014)	PBS-10% NGS-3% BSA-0.4% TX	Anti-rat Alexa Fluor 594 (1:500) Life Technologies
Rabbit anti-CGRP (1:1000) Sigma C8198	Ciglieri et al. (2016)	PBS–5% NGS	Anti-rabbit Alexa Fluor 488/633 (1:500) Life Technologies
IB4-biotin conjugate (1:250) Sigma L2140	Bencivinni et al. (2011)	PBS–6% BSA	ExtrAvidin CY3(1:1000) ExtrAvidin FITC (1:250) Sigma

BSA bovine serum albumin, *CGRP* calcitonin gene-related peptide, *GFP* green fluorescent protein, *GINIP* Gα inhibitory interacting protein, *IB4* isolectin B4, *NGS* normal goat serum, *PBS* phosphate-buffered saline, *TRPV1* transient receptor potential vanilloid 1, *TX* triton X-100, *VGLUT3* vesicular glutamate transporter 3

*Pre-absorption tests performed in this work:

Anti-VGLUT3 antibody pre-absorption with different concentrations of a 16-residue synthetic peptide derived from C terminal domain of rat VGLUT3 (1–100 µg/ml) resulted in a dose-dependent decrease of immunolabeling that was completely abolished at 25 µg/ml

Anti-TRPV1 antibody pre-absorption with different concentrations of the immunogenic peptide (C)EDAEVFKDSMVPGEK corresponding to amino acid residues 824–838 of rat TRPV1 (1–100 µg/ml) resulted in a dose-dependent decrease of immunolabeling that was completely abolished at 1.5 µg/ml

Quantification and Statistical Analysis

LM Quantification of Immunoreactive DRG Neurons

Twelve lumbar DRGs from TAFA4^{Venus} mice ($n = 3$) and twelve lumbar DRGs from CD1 mice ($n = 3$) were serially sectioned in toto at 10 µm. One out of five sections in the series was immunostained, thus minimizing the risk of double-counting the same neuron and allowing the analysis of the entire ganglion. Individual sections were triple-immunostained with one of the following combinations of markers: GFP+VGLUT3+IB4; GINIP+VGLUT3+IB4; GINIP+CGRP+IB4; VGLUT3+CGRP+IB4; TRPV1+CGRP+IB4; TRPV1+VGLUT3+GINIP. Single-, double- or triple-labeled DRG neurons were directly counted from fluorescence images with the software Adobe Photoshop CS2 9. Results were expressed as mean (± SEM) number of cells/DRG or as mean percentages (± SEM) of double-labeled neurons vs the total number of single-labeled cells for each combination of multiple antigens, with n indicating the number of mice. To test homogeneity of variance across DRG samples, the Levene's test for equality of variances was used. Variances were considered different for $p < 0.05$.

LM Quantification of Immunoreactive Non-peptidergic Primary Afferent Fibers (PAFs) from GINIP Mice

Spinal cord sections triple-immunostained for TRPV1+GINIP+IB4 were observed at the confocal microscope. Laser parameters were unchanged for the two different experimental conditions (controls vs DT) so that the detection of staining was maximal, while avoiding pixel saturation. Ten randomly selected sections/animal were analyzed with the ImageJ software (NIH, Bethesda, MD, USA) by an operator unaware of the experimental group.

Mean fluorescence intensity (MFI), the fluorescent dorsal horn (lamina II) area (FDHA) and fluorescence-integrated density (FID) were measured. MFI was estimated by subtracting the background mean value from the overall mean grey value. FID was calculated as MFI × FDHA.

EM Quantification of Glomeruli in GINIP Mice

We counted the number of glomeruli in lamina II to assess whether there was a loss after DT-selective ablation of GINIP-expressing neurons. Glomeruli are known to occur in two main types, each, in turn, existing in two different configurations (see Ribeiro-da-Silva 2015). Type Ia glomeruli

Table 2 Antibodies and spinal cord preparation for transmission electron microscopy

Primary antibodies or biotin-conjugate	Donors	Embedding	Immunostaining	Secondary antibodies
Chicken anti-GFP (1:20) Aves Labs GFP-1020	TAFA4^{Venus} mice	LR white acrylic resin (Sigma, St. Louis, MO, USA) to preserve GFP antigenicity Luby-Phelps et al. (2003); Kambrun et al. (2018)	Post-embedding immunogold Merighi and Polak (1993)	Anti-chicken antibody 10-nm gold conjugated (1:15) BBI solutions
Rabbit anti-VGLUT3 (1:20) Abcam ab23977	CD1, GINIP, TAFA4^{Venus} mice	Spurr epoxy resin (Electron Microscopy Sciences, Hatfield, PA, USA) for CD1 and GINIP mice Calorio et al. (2019) LR white acrylic resin (Sigma) for TAFA4^{Venus} mice Luby-Phelps et al. (2003); Kambrun et al. (2018)	Post-embedding immunogold Merighi and Polak (1993)	Anti-rabbit antibody 30-nm gold conjugated (1:15) BBI solutions
Rabbit anti-TRPV1 (1:500) Alomone ACC-030	CD1, GINIP, TAFA4^{Venus} mice	Spurr epoxy resin (Electron Microscopy Sciences,) for CD1 and GINIP mice Calorio et al. (2019) LR white acrylic resin (Sigma) for TAFA4^{Venus} mice Luby-Phelps et al. (2003); Kambrun et al. (2018)	Pre-embedding FluoroNanogold on free-floating vibratome sections Salio et al. (2011)	Anti-rabbit biotinylated antibody (1:200), Vector+AlexaFluor 488-Fluoronanogold-Streptavidin (1:100), Nanoprobes
Rat anti-GINIP (1:20) Gaillard et al. (2014)	CD1, GINIP, TAFA4^{Venus} mice	Spurr epoxy resin (Electron Microscopy Sciences) for CD1 and GINIP mice Calorio et al. (2019) LR white acrylic resin (Sigma) for TAFA4^{Venus} mice Luby-Phelps et al. (2003); Kambrun et al. (2018)	Post-embedding immunogold Merighi and Polak (1993)	Anti-rat antibody 10-nm gold-conjugated (1:15) BBI solutions
IB4-biotin conjugate (1:20) Sigma L2140	CD1, GINIP, TAFA4^{Venus} mice	Spurr epoxy resin (Electron Microscopy Sciences) for CD1 and GINIP mice Calorio et al. (2019) LR white acrylic resin (Sigma) for TAFA4^{Venus} mice Luby-Phelps et al. (2003); Kambrun et al. (2018)	Post-embedding immunogold Merighi and Polak (1993)	Streptavidin 20-nm gold-conjugated (1:15) Sigma

Sections, immunostained for TRPV1 with the FluoroNanogold protocol, were then labeled for VGLUT3, IB4, GINIP, and GFP using conventional post-embedding immunogold staining

GFP green fluorescent protein, *GINIP* Gα inhibitory interacting protein, *IB4* isolectin B4, *TRPV1* transient receptor potential vanilloid 1, *VGLUT3* vesicular glutamate transporter 3

(GIa) are known to arise from non-peptidergic PAFs. Therefore, we focused our analysis on counting GIa from control vs DT animals in (i) plain ultrathin sections; and (ii) sections immunolabeled for GINIP, IB4 and VGLUT3. However, being previously reported that VGLUT3^{+} C-LTMRs were engaged in type II glomeruli (GII) in both rat and mouse (Larsson and Broman 2019) and that GINIP was expressed in almost 30% of peptidergic DRG neurons in rat (Liu et al. 2016), quantification of GII and peptidergic type Ib glomeruli (GIb) was also performed.

For a more precise quantification, since IB4^{+} afferents innervating the most lateral part of the spinal dorsal horn were still present after DT injection in previous IMF studies (Urien et al. 2017), lamina II was divided into a medial and lateral part of equal wideness after observation of toluidine blue-stained semi-thin sections at the light microscope. Ten

sections/animal for control (medial and lateral part; $n=3$) and 10 sections/animal for DT (medial and lateral part; $n=3$) mice were examined in studies that were carried out by an operator unaware of the experimental group. More precisely, the experimenter directly counted the number of glomeruli within all the 90×90 µm squares of 200 mesh EM grids that were occupied by relevant tissue. Quantitative analysis was performed using the ImageJ software (NIH, Bethesda, USA) and Graph Pad Prism 6 (GraphPad Software, San Diego, CA, USA). Differences were evaluated with non-parametric Mann–Whitney test, and considered significant for $p<0.05$.

Results

IB4 Labeling and TAFA4 Immunoreactivity Identify Two Distinct Subpopulations of Mouse Non-peptidergic C-type DRG Neurons

As the mouse C-type non-peptidergic DRG neurons have been distinguished into two main subpopulations of VGLUT3$^+$/TAFA4$^+$ C-LTMRs and IB4$^+$ C-Ncs, we have first established the pattern of coexistence of these markers in TAFA4/VGLUT3/IB4 triple-labeling experiments and then calculated the relative abundance of the two subpopulations of neurons in lumbar DRGs. All labeled neurons were of small size, and thus, histologically, could be positively identified as C-type neurons (IB4$^+$ neurons < 20 µm diameter, average 18.5 ± 0.2 µm; TAFA4$^+$ neurons: < 20 µm diameter, average 18 ± 0.2 µm; VGLUT3$^+$ neurons: < 20 µm diameter, average 18.7 ± 1.2 µm). The percentages of co-expression of TAFA4 and VGLUT3 were above 90% (VGLUT3$^+$ vs TAFA$^+$: 95.5 ± 0.4%; TAFA4$^+$ vs VGLUT3$^+$: 90.1 ± 0.8%). Thus, if one considers the inherent technical drawbacks associated with the use of multiple immunostaining techniques, it seems reasonable to held that the two molecules coexisted in all C-LTMRs. On the other hand, the DRG neurons labeled for IB4 formed, as expected, a fully separate subpopulation (Fig. 1a–d).

Given the coexistence of VGLUT3 and TAFA4, and the absence of IB4/VGLUT3 double-stained neurons, we counted VGLUT3$^+$ and TAFA4$^+$ neurons to measure the number of C-LTMRs/DRG and to calculate their relative abundance compared to the IB4$^+$ C-Ncs. We thus observed that the IB4$^+$ neurons resulted 3.5 times more numerous than those expressing VGLUT3 (500.3 ± 3.3 IB4$^+$ cells/DRG vs 140.6 ± 1.45 VGLUT3$^+$ cells/DRG) and 3.4 times more abundant than those expressing TAFA4 (500.3 ± 3.3 IB4$^+$ cells/DRG vs 146.6 ± 1.6 TAFA4$^+$ cells/DRG). The variances in numbers for IB4$^+$, VGLUT3$^+$ and TAFA4$^+$ DRG neurons sampled from the ganglia of three different mice were not statistically different at the Levene's test ($P=0.93$, $P=0.52$ and $P=0.57$, respectively) indicating homogeneity in the samples, and hence, the absence of individual variations.

In another set of triple-labeling experiments, we investigated the coexistence of the IB4, VGLUT3 and GINIP labels in single DRG neurons (Fig. 1e–h). As predictable, VGLUT3$^+$ and IB4$^+$ DRG neurons also expressed GINIP. The degree of co-expression of VGLUT3 and GINIP was so high (97.8 ± 0.2%) that, again, one could safely conclude that the two markers coexisted in all C-LTMRs. The percentage of IB4/GINIP double-labeled DRG neurons was also high (IB4$^+$ vs GINIP$^+$: 77.7 ± 0.2%), but about one-fourth of the GINIP-expressing neurons were not stained by IB4. To confirm that the VGLUT3$^+$ neurons were not peptidergic and to ascertain if the IB4$^-$/GINIP$^+$ neurons could be peptidergic, we performed another series of multiple labeling experiments leading us to conclude that neither GINIP$^+$ (Fig. 1i–l) nor VGLUT3$^+$ DRG neurons (Fig. 1m–p) co-expressed the peptidergic marker CGRP.

TRPV1 is Expressed in Peptidergic CGRP$^+$ and a Small Percentage of Non-peptidergic IB4$^+$ C-type DRG Neurons and their PAFs Projecting to Laminae I–II of the Dorsal Horn

We then investigated the pattern of expression of TRPV1 in C-type DRG neurons by performing triple-labeling experiments with the anti-TRPV1 antibody, the anti-CGRP antibody and the IB4-biotin conjugate. As expected, TRPV1 was co-expressed with CGRP in a large percentage of these neurons (TRPV1$^+$/CGRP$^+$: 88.5 ± 0.7%; CGRP$^+$/TRPV1$^+$: 56.8 ± 0.7%; n = 3 mice; Fig. 2a, b, d). However, a small percentage of IB4$^+$ non-peptidergic C-type neurons also expressed TRPV1 (IB4$^+$/TRPV1$^+$: 3.6 ± 0.2%; TRPV1$^+$/IB4$^+$: 11 ± 0.2%; $n=3$ mice; Fig. 2a, c, d). In another set of experiments, we showed that TRPV1 was never expressed in TAFA4$^+$ (Fig. 2e, f, h) or in GINIP$^+$ neurons (Fig. 2e, g, h).

At the spinal cord level, the pattern of expression of TRPV1 was fully consistent with the above observations in DRGs. TRPV1 and CGRP co-expression occurred in lamina I and II outer (II_o; Fig. 2i). TRPV1$^+$ non-peptidergic IB4$^+$ C-fibers were, instead, localized in a band at the border between lamina II_o and the dorsal part of inner lamina II (II_{id}) (Fig. 2i, j). Finally, TRPV1 and TAFA4 immunoreactive PAFs occupied the two subdivisions of lamina II_i, with the former in II_o–II_{id} and the latter in II_{iv} (Fig. 2j), at the border with lamina III.

Non-peptidergic C-LTMRs and C-Ncs in Lamina II form the Central Boutons of GIa but No Other Types of Glomeruli or Axo-Dendritic Synapses

TEM experiments confirmed the concomitant presence of TAFA4/VGLUT3 (Fig. 2k) and TRPV1/IB4 staining

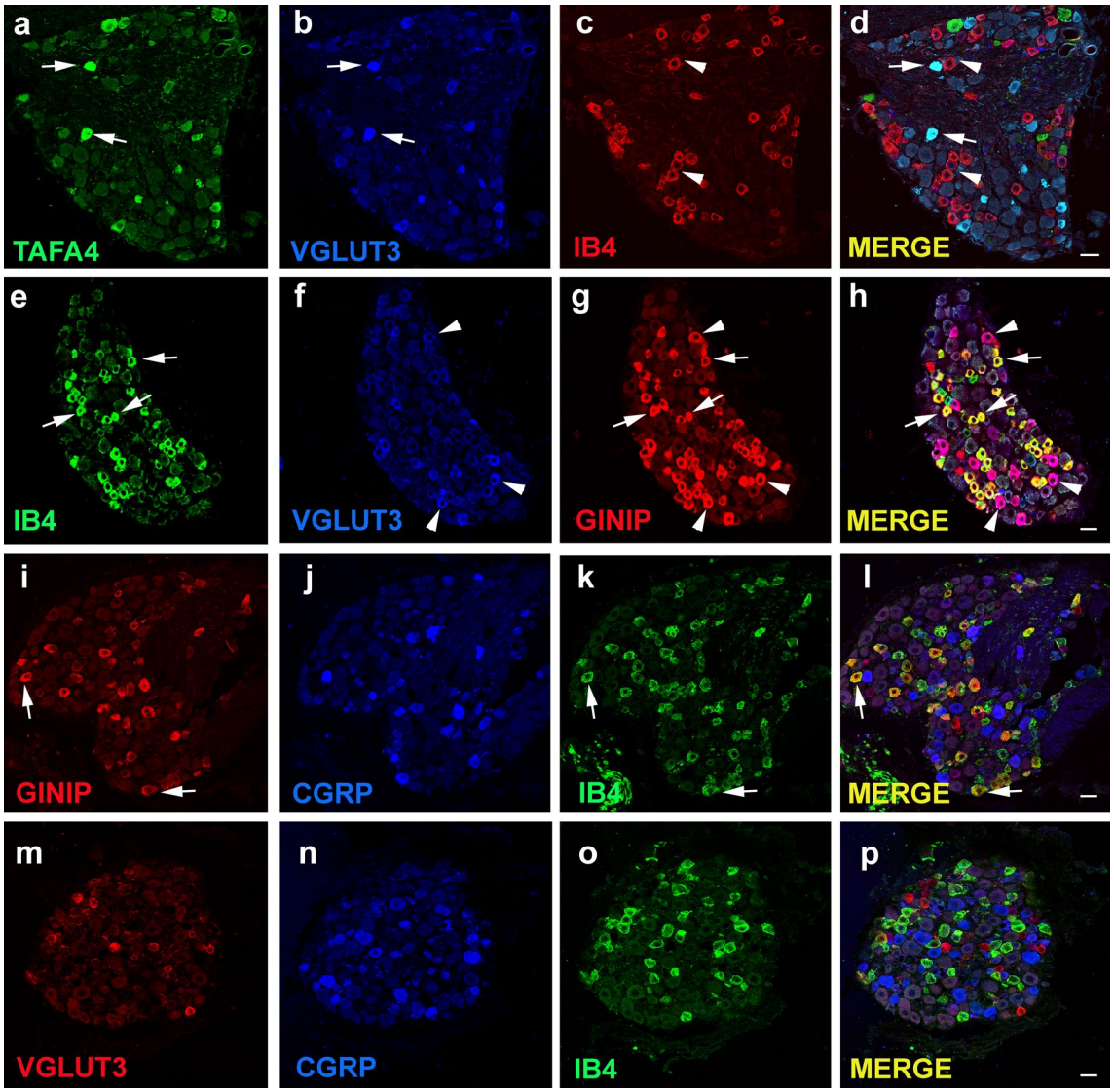

Fig. 1 Neurochemical characterization of non-peptidergic C-type DRG neurons. **a**–**d** GFP, used to detect the TAFA4$^+$ Venus fusion protein (**a**, green) and VGLUT3, used as a marker of C-LTMRs (**b**, blue), are highly co-expressed in small-sized non-peptidergic DRG neurons (**d**, light blue), while IB4 (**c**, **d**, red) labels a different population of small-sized non-peptidergic neurons. As an example, the arrows indicate two TAFA4$^+$/VGLUT3$^+$ neurons, whereas the arrowheads point to two neurons that are singularly labeled by IB4. **e**–**h** Both IB4$^+$ (**e**, green) and VGLUT3$^+$ (**f**, blue) small-sized non-peptidergic DRG neurons also express GINIP (**g**, red) as shown in **h** (yellow and fuchsia, respectively). The arrows and arrowheads point to some IB4$^+$/GINIP$^+$ and VGLUT3$^+$/GINIP$^+$ neurons, respectively. **i**–**l** GINIP (**i**, red) is not co-expressed with CGRP (**j**, **l**, blue) in small-sized peptidergic DRG neurons, but coexists with IB4 (**k**, green; **l**, yellow, arrows) in non-peptidergic neurons. **m**–**p** VGLUT3 (**m**, red) is not expressed in CGRP$^+$ (**n**, **p**, blue) or IB4$^+$ (**o**, **p**, green) small-sized DRG neurons. Scale bars: 50 µm

(Fig. 2l) in non-peptidergic PAF terminals. These terminals were engaged in GIa that today we know to originate specifically from non-peptidergic C-fibers (Ribeiro-da-Silva 2015). In rat, GIa are exclusive to lamina II, and chiefly prominent in II_{id} (Ribeiro-da-Silva and De Koninck 2008). Thus, ultrastructural observations were valuable to confirm beyond doubts the nature and functional properties of the VGLUT3/TAFA4 and TRPV1/IB4 labeled PAFs.

Finally, it is worth mentioning that simple axo-dendritic synapses in lamina II were consistently unlabeled.

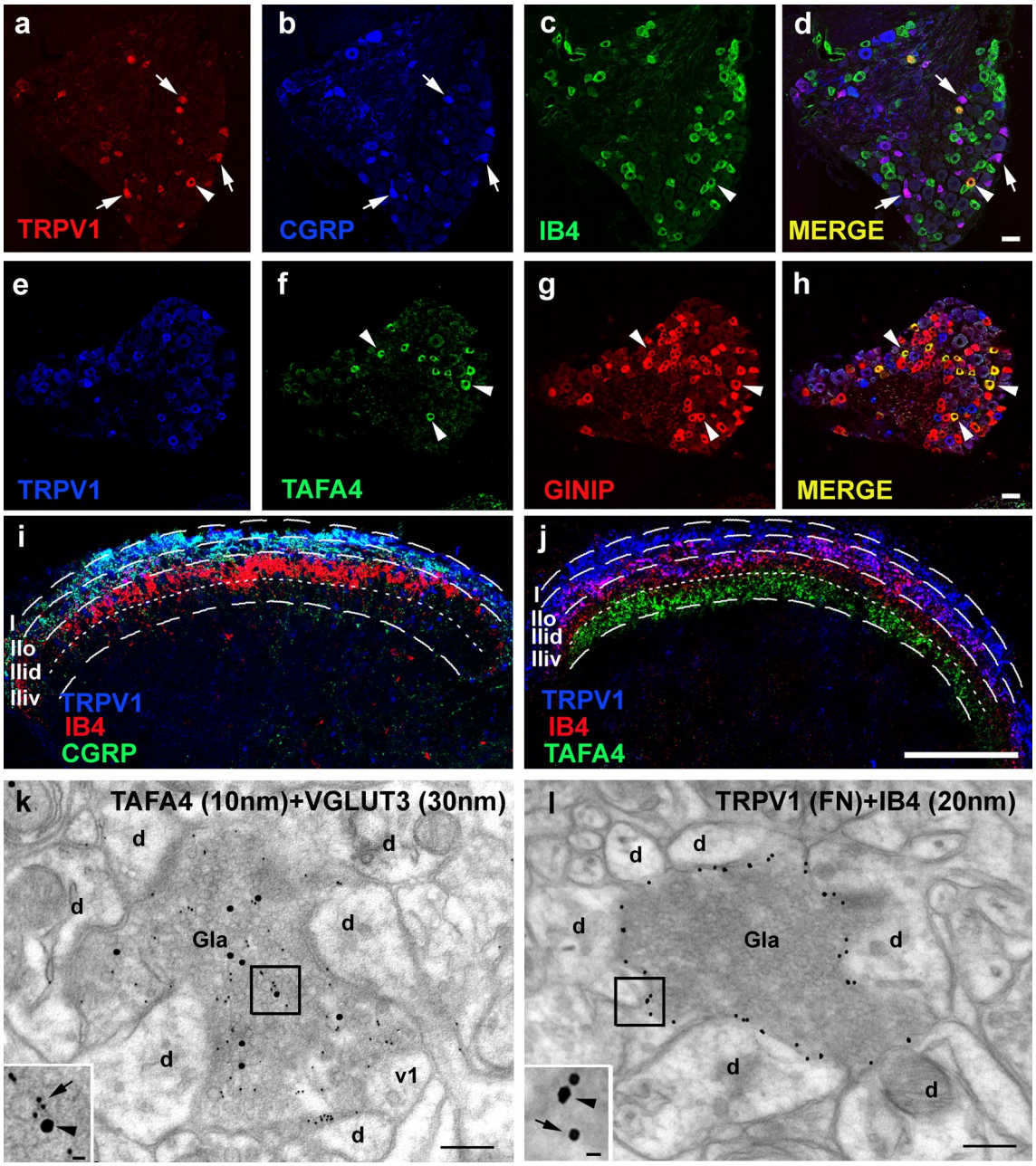

Fig. 2 TRPV1 expression in CGRP$^+$ peptidergic and IB4$^+$ non-peptidergic DRG neurons and PAFs projecting to laminae I–II of the dorsal horn. **a**–**d** TRPV1 (**a**, red) is highly co-expressed with CGRP (**b**, blue; **d**, fuchsia, arrows) in small-sized peptidergic DRG neurons, while occasional TRPV1$^+$ small-sized non-peptidergic neurons are also IB4$^+$ (**c**, green; **d**, yellow, arrowhead). **e**–**h** TRPV1 (**a**, blue) is not co-expressed with TAFA4 (**f**, green) or GINIP (**g**, red), while TAFA4$^+$ (**f**, green) small-sized non-peptidergic DRG neurons also express GINIP (**g**, red) as shown in **h** (yellow; arrowheads). **i** TRPV1 (blue) and CGRP (green) are extensively co-expressed in PAFs distributed in lamina I and II_o (light blue merge), while TRPV1 (blue) and IB4 (red) are only co-expressed (fuchsia merge) in a small population of PAFs distributed in a band at the border between lamina II_o and the dorsal part of inner lamina II (II_{id}). **j** TRPV1 (blue) and TAFA4 (green) are not co-expressed in PAFs, with TRPV1 distributed in laminae I–II_o and TAFA4 in II_{iv}. TRPV1 (blue) and IB4 (red) co-express in PAFs laying at the border between II_o and II_{id} (fuchsia). **k** Several unlabeled dendrites (d) and a vesicle-containing dendrite (v1) are engaged in a GIa with the central bouton double-labeled for TAFA4 and VGLUT3. The immunogold signal is scattered over the small clear synaptic vesicles. The area in the square is enlarged in the insert (the arrow points to a cluster of three 10-nm gold particles; the arrowhead to a 30-nm gold particle). **l** a TRPV1$^+$/IB4$^+$ double-labeled terminal in GIa is surrounded by a few unlabeled dendrites (d). Both gold labels (30-nm intensified gold particles of irregular shape for TRPV1 and plain 20-nm gold particles for IB4) are localized over the terminal axolemma. The area in the square is magnified in the insert, where the arrowhead points to a gold-intensified particle and the arrow to one of the two 20-nm gold particles of regular shape. Scale bars: **a**–**h**: 50 µm; **i**, **j**: 200 µm; **k**, **l**: 250 nm; insets: 30 nm

The Selective Ablation of GINIP-Expressing Sensory Neurons in DRGs Does Not Affect TRPV1$^+$ Non-peptidergic PAFs but Reduces IB4$^+$ Non-peptidergic PAFs Predominantly in the Medial Part of Lamina II

To investigate further the coexistence of GINIP in specific subpopulations of C-type non-peptidergic fibers and ascertain whether TRPV1 was indeed present in IB4$^+$ C-Ncs, we performed experiments on engineered *ginip* mice (Fig. 3). These experiments revealed that DT treatment was effective in abolishing almost completely GINIP immunostaining in the superficial dorsal horn (Fig. 3a), but not the TRPV1 signal (Fig. 3a). In addition, when TRPV1/GINIP/IB4 triple-labeled preparations were subjected to quantitative analysis of IMF (Fig. 3b), FID and FDHA for TRPV1 immunoreactivity were unchanged after DT administration (FID: CTR: 457528 ± 1347.73; DT: 469877 ± 39.70; Mann–Whitney test, $p = 0.1021$; FDHA: CTR: 21069 ± 160.13; DT: 20755 ± 29.23; Mann–Whitney test, $p = 0.7441$), whereas the GINIP signal was significantly reduced. Therefore, we concluded that GINIP$^+$ non-peptidergic PAFs did not express TRPV1. In these experiments, we also observed that not all IB4$^+$ PAFs disappeared after the ablation of GINIP and that surviving fibers were particularly abundant in the lateral part of the dorsal horn as clearly seen at the fluorescence microscope (Fig. 3a) and after quantitative analysis (Fig. 3b).

Selective Ablation of GINIP-Expressing Sensory Neurons Affects the Non-peptidergic C-LTMRs Glomerular Terminals in Lamina II

Given that we have observed the existence of a DT-resistant subpopulation of IB4-stained fibers in lamina II, we have counted GIa to better characterize the alterations determined by the DT injection. First, we have considered the absolute number of GIa in plain, not-immunostained sections. Of note, GIa resulted to be more concentrated in the lateral part of lamina II, and after DT, glomeruli diminished to 55.4% of those in control mice (Fig. 4a). However, consistently with IMF observations, the numerical ratio of GIa in the lateral vs the medial lamina II raised from 1.24 in control mice to 1.91 after DT. This observation confirmed that at least part of the non-peptidergic C-fibers in lateral lamina II were resistant to DT, likely because they did not express GINIP as there were many IB4$^+$/GINIP$^-$ neurons in DRGs (see Fig. 1i–l). We also calculated the density of GIa (number of GIa/section—Fig. 4b) and, again, observed a numerical

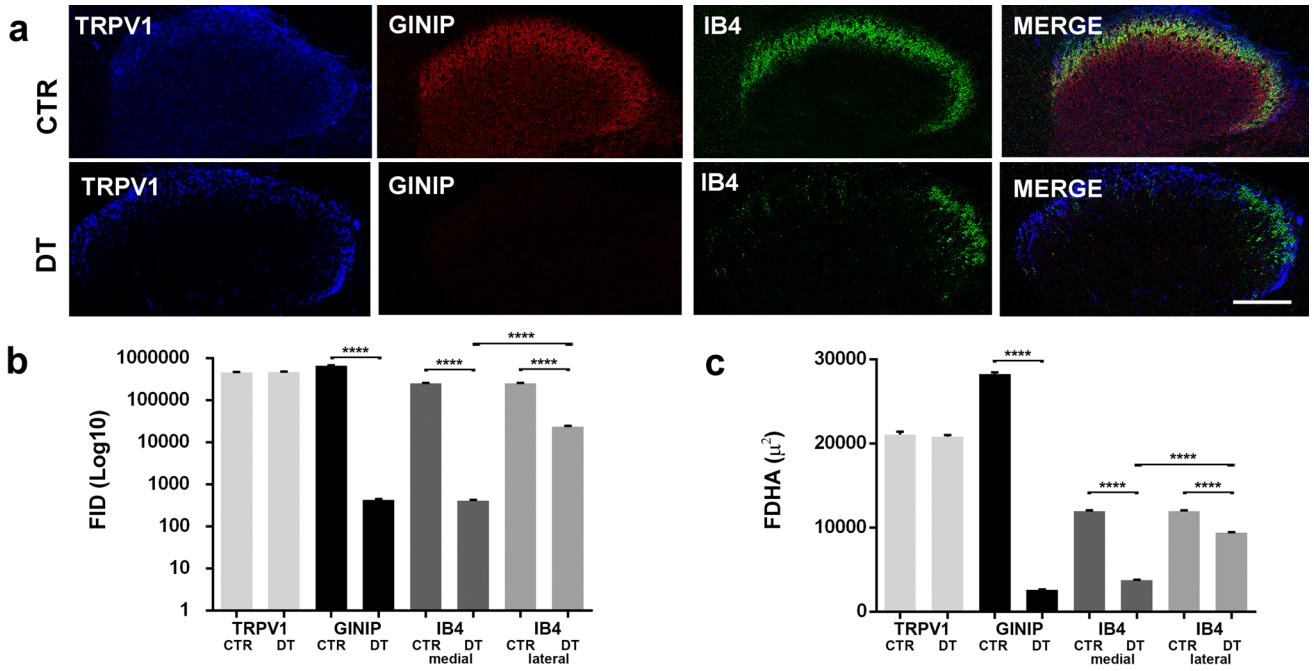

Fig. 3 TRPV1 expression in non-peptidergic PAFs after DT treatment. **a** Spinal cord sections from control (CTR) and GINIP-ablated (DT) mice, labeled for TRPV1 (blue), GINIP (red) and IB4 (green). TRPV1 immunoreactive fibers are not affected by DT injection. After DT treatment, GINIP immunostaining completely disappears and IB4 labeling principally persists in the lateral part of the dorsal horn. **b** Histogram illustrating the fluorescence-integrated density (FID) in CTR vs DT mice for TRPV1 (light grey bar, Mann–Whitney test, $p = 0.1021$), GINIP (black bar, Mann–Whitney test, $p < 0.0001$), IB4 medial (dark grey bar, Mann–Whitney test, $p < 0.0001$) and IB4 lateral (grey bar, Mann–Whitney test, $p < 0.0001$). **c** Bar chart illustrating the fluorescent dorsal horn area (FDHA) in CTR vs DT mice for TRPV1 (light grey bar, Mann–Whitney test, $p = 0.7441$), GINIP (black bar, Mann–Whitney test, $p < 0.0001$), IB4 medial (dark grey bar, Mann–Whitney test, $p < 0.0001$) and IB4 lateral (grey bar, Mann–Whitney test, $p < 0.0001$). Scale bar: a: 200 µm

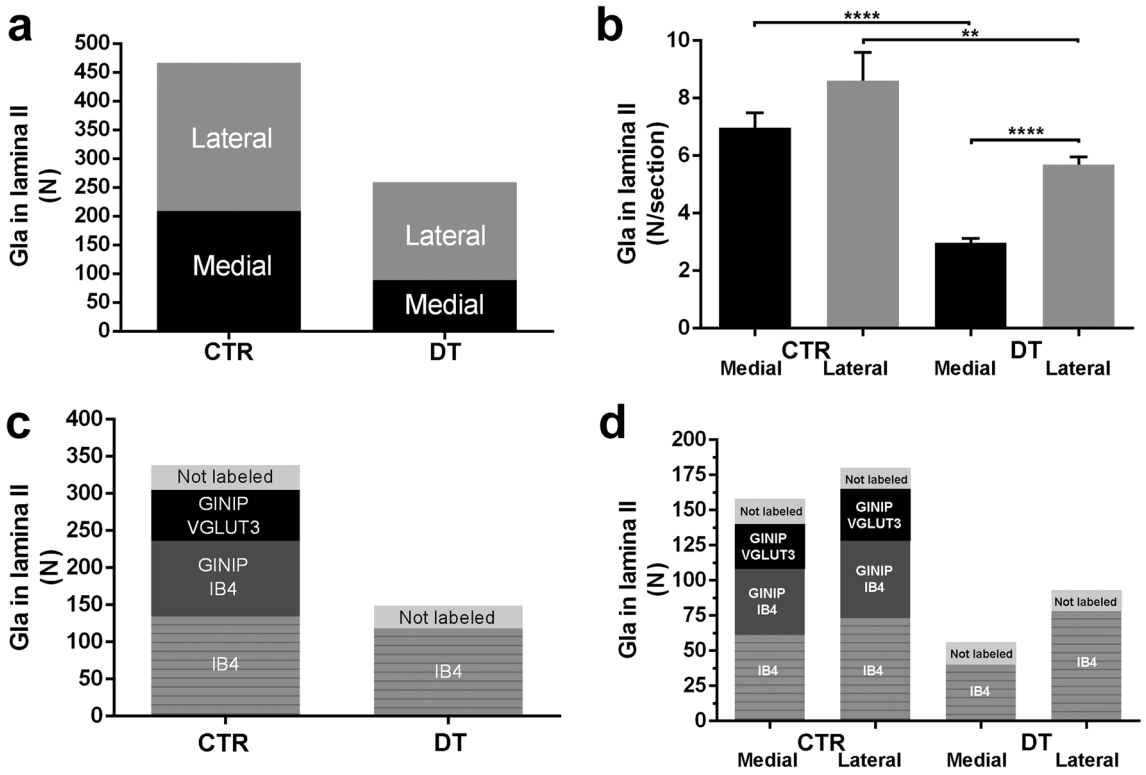

Fig. 4 Numerical changes of non-peptidergic GIa after DT treatment. **a** Histogram illustrating the total number of Gla glomeruli counted in lamina II ($N=467$ in CTR; $N=259$ after DT). GIa are more concentrated in the lateral part of lamina II both in CTR ($N=258$ lateral, $N=209$ medial), and after DT ($N=170$ lateral, $N=89$ medial). **b** Histogram showing the number of GIa/section in the medial and lateral part of lamina II. A statistically significant reduction of GIa density is seen after DT vs CTR both in the medial (Mann–Whitney test, $p<0.0001$) and lateral part of lamina II (Mann–Whitney test, $p=0.0035$). **c** Histogram illustrating the total number of immunolabeled Gla glomeruli in lamina II ($N=338$ in CTR and $N=149$ after DT). CTR: IB4$^+$ ($N=134$), GINIP$^+$/IB4$^+$ ($N=102$), GINIP$^+$/VGLUT3$^+$ ($N=69$) labeled GIa and not labeled GIa ($N=33$). DT: IB4$^+$ GIa ($N=118$) and not labeled GIa ($N=31$). **d** Histogram illustrating the total number of immunolabeled Gla glomeruli counted in the medial and lateral part of lamina II. In CTR, the different types of immunolabeled GIa show a similar distribution in the medial and lateral part of lamina II, while after DT IB4$^+$ GIa in the lateral part are almost double than in the medial one

reduction after DT. Decrease was statistically significant in both the medial (57.4% reduction; Mann–Whitney test, $p<0.0001$) and lateral (33.7% reduction; Mann–Whitney test, $p=0.0035$) part of lamina II, but with a clearly much minor effect in the latter.

We have then performed a series of GINIP/IB4/VGLUT3 triple-labeling experiments to quantitate the relative contribution of the different subpopulations of C-type non-peptidergic fibers to the total number of GIa in lamina II. After these experiments, the total number of GIa in lamina II of DT-treated mice was 45% of that in untreated controls (Fig. 4 c), but their density was not statistically changed (CTR: Mann–Whitney test, $p=0.4$; DT: Mann–Whitney test, $p=0.1$). Of these, in CTR (Figs. 4c, 5a) we observed a prevalence of IB4$^+$ GIa ($N=134$; 39.6%), followed by GINIP$^+$/IB4$^+$ GIa ($N=102$; 30.2%), GINIP$^+$/VGLUT3$^+$ GIa ($N=69$; 20.4%), and unlabeled GIa ($N=33$; 9.8%). In DT, as expected, we detected a complete loss of GINIP$^+$/VGLUT3$^+$ and GINIP$^+$/IB4$^+$ GIa ($N=69$ in CTR and $N=0$ in DT, Figs. 4c, 5b), while IB4$^+$ GIa ($N=118$; 79.2%; Figs. 4c, 5b) and unlabeled GIa ($N=31$; 20.8%; Fig. 4c) were unaffected. It is worth remarking that the absolute number of glomeruli in the two DT-insensitive subpopulations (singularly labeled IB4$^+$ and unlabeled) was similar in treated and untreated mice, with ratios of 0.88 and 0.94, respectively. It is also relevant that, in CTR, the different type of labeled GIa showed a comparable distribution in the medial and lateral part of lamina II (Fig. 4d), while, after DT, IB4$^+$ GIa were almost doubled in the lateral part of lamina II (Fig. 4d). This is a remarkable finding as it suggests that there is very little plasticity or reorganization of the projection patterns of the surviving terminals.

Of note, GIb and GII were consistently negative for GINIP, VGLUT3, or IB4 in control and DT-treated mice.

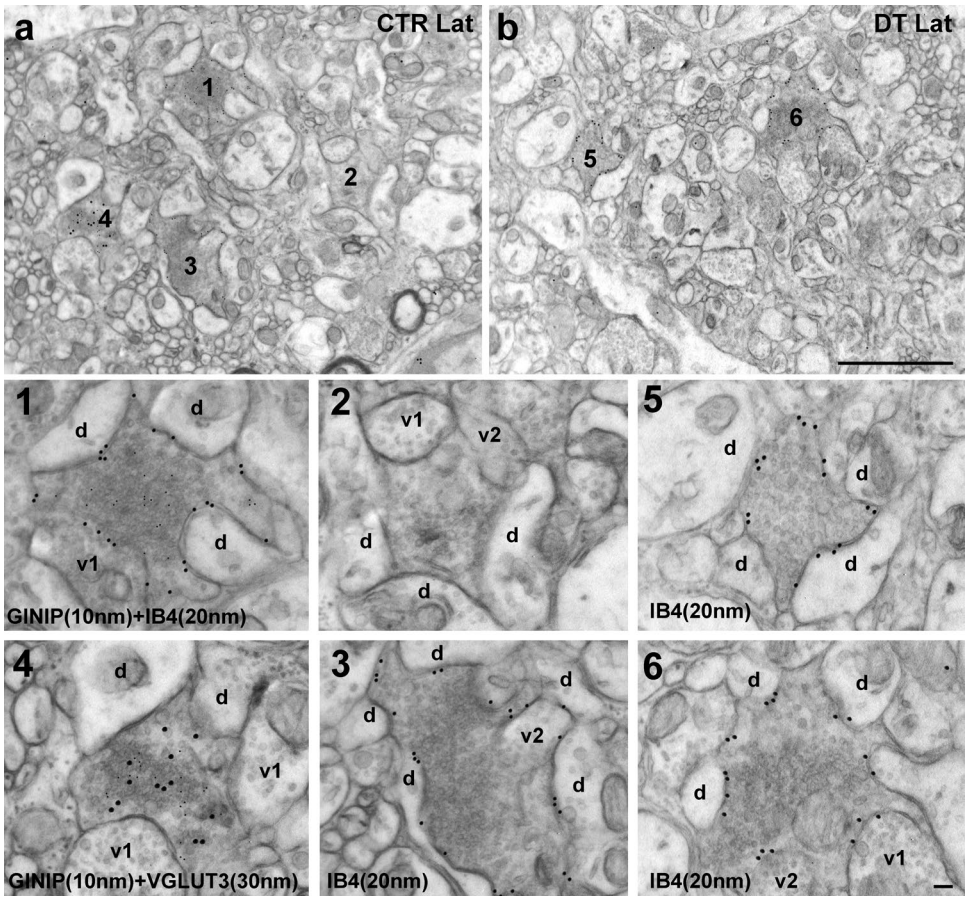

Fig. 5 Ultrastructure of non-peptidergic C-Ncs and C-LTMRs in lamina II of CTR and DT-treated mice **a** Top, low-magnification electron micrograph showing four GIa in the lateral part of lamina II in CTR mice. Bottom, high-magnification images corresponding to GIa numbered 1–4 in **a**, showing a GINIP$^+$/IB4$^+$ GIa (**1**), an unlabeled GIa (**2**), a IB4$^+$ GIa (**3**) and a GINIP$^+$/VGLUT3$^+$ GIa (**4**). **b** Top, low-magnification electron micrograph showing a few GIa in the lateral part of the spinal lamina II after DT. Bottom, high-magnification images corresponding to GIa numbered 5–6 in **b**, both labeled for IB4. Scale bars: **a**, **b**: 2 µm; 1–6: 100 nm

Discussion

We here studied the immunocytochemistry of the mouse C-type DRG neurons and their central terminals in lamina II of the dorsal horn at light and electron microscopic levels. We used a panel of markers (CGRP, IB4, TRPV1 and VGLUT3), and two genetically modified mouse models to provide an exhaustive neurochemical characterization of these neurons, focusing onto C-Ncs and C-LTMRs.

We first observed that GINIP, differently from rat (Liu et al. 2016), was not expressed in mouse by the peptidergic C-Ncs, which were unlabeled with IB4 but CGRP$^+$ and TRPV1$^+$. These TRPV1$^+$/CGRP$^+$/IB4$^-$ murine neurons were previously proven to be heat-specific cutaneous nociceptors (Lawson et al. 2008), in agreement with earlier mouse studies that showed a high degree of coexistence of TRPV1 and CGRP in C-type DRG neurons (Zwick et al. 2002; Woodbury et al. 2004). Still in mouse, after inducing a degeneration of these cells and their cutaneous fibers, these initial findings were reinforced by observing that the peptidergic TRPV1$^+$ DRG neurons were completely (substance P$^+$) or partly (CGRP$^+$) depleted, with the onset of thermal hypoalgesia (Hsieh et al. 2012).

We then noticed that murine non-peptidergic C-type DRG neurons could be subdivided into three different subpopulations: two types of C-Ncs with different neurochemical features (IB4$^+$/GINIP$^+$/TRPV1$^-$ or IB4$^+$/GINIP$^-$/TRPV1$^+$) and the C-LTMRs expressing VGLUT3, TAFA4, and GINIP (Fig. 6).

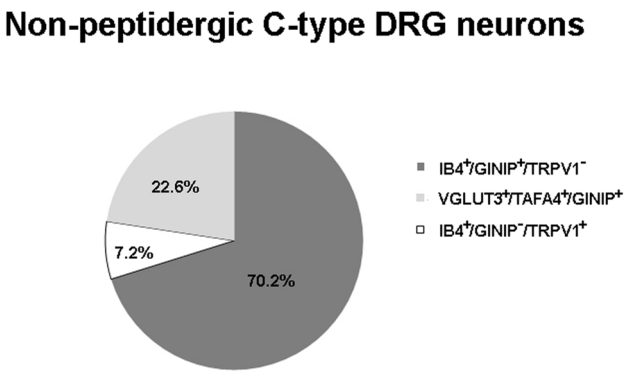

Fig. 6 Subpopulations of non-peptidergic C-type DRG neurons. The pie chart shows the percentage of expression of IB4$^+$/GINIP$^+$/TRPV1$^-$ C-Ncs (dark gray; 70.2%), VGLUT3$^+$/TAFA4$^+$/GINIP$^+$ C-LTMRs (light gray; 22.6%) and IB4$^+$/GINIP$^-$/TRPV1$^+$ C-Ncs (white; 7.2%)

It is well established that the mouse IB4$^+$ non-peptidergic C-Ncs (Silverman and Kruger 1990; Ruscheweyh et al. 2007) give rise to cutaneous free nerve endings (Gaillard et al. 2014; Reynders et al. 2015). Although the terminal morphology of these fibers clearly speaks in favor of their nociceptive role, it is much less clear whether these neurons express other putative nociceptive/non-nociceptive markers, and thus, might form functionally different subgroups. Thus, it is of interest that we here reinforced the belief that the mouse non-peptidergic IB4$^+$ C-Ncs indeed formed two separate subpopulations, respectively expressing GINIP *or* TRPV1, in line with previous observations (Gaillard et al. 2014).

We will discuss the specific features of these two emerging classes of murine non-peptidergic C-Ncs and then the new information related to mouse C-LTMRs that could be gathered from the observations of this study.

GINIP$^+$/IB4$^+$/TRPV1$^-$ Non-peptidergic C-Ncs

We have here calculated that IB4$^+$/GINIP$^+$/TRPV1$^-$ DRG neurons represented more than 90% of non-peptidergic IB4$^+$ C-Ncs. Lawson et al. (2008) have shown that a large proportion of the mouse polymodal C-type DRG neurons responding to mechanical and heat stimuli were IB4$^+$ but negative for TRPV1. Therefore, it is conceivable that the IB4$^+$/GINIP$^+$/TRPV1$^-$ DRG neurons are polymodal non-peptidergic C-Ncs. Yet, Gaillard et al. (2014) have proven that GINIP null mice exhibited a selective and prolonged injury-induced mechanical hypersensitivity, but no obvious behavioral alterations after thermal testing. Then, in a subsequent study, Urien et al. (2017) have demonstrated that the genetic ablation of the GINIP-expressing DRG neurons impaired the formalin-evoked pain, likely due to a specific loss of the GINIP$^+$ neurons that do not bind IB4. Thus, there is a clear discrepancy between the study of Lawson et al. (2008) from one side and those of Gaillard et al. (2014) and Urien et al. (2017) from the other; as from these findings, it appears that different types of stimuli (thermal versus mechanical/chemical) can activate GINIP$^+$/IB4$^+$/TRPV1$^-$ non-peptidergic C-Ncs. The reason of such a discrepancy remains to be determined in full. Yet, as a possible explanation, one must consider that an ex vivo somatosensory system preparation was used by Lawson et al. (2008), whereas transgenic mice were employed in the other two studies.

To achieve more information about this class of non-peptidergic C-Ncs, we have experimentally depleted them in the *ginip* conditional model. At LM, we have thus observed that the ablation of GINIP resulted in a strong reduction of IB4 labeling in the medial part of lamina II, but only affected minimally the lateral lamina II. These IMF observations were consistent with those at the ultrastructural level where, after DT treatment, the surviving IB4$^+$ GIa were almost twofold more numerous in the lateral lamina II compared to its medial half. These two series of experiments showed that the GINIP$^+$/IB4$^+$ C-Ncs displayed an uneven spread along the transversal axis of the spinal cord, with prevalence in its medial half.

Cruz et al. (1987), after horseradish peroxidase (HRP) tracing and Golgi impregnation, were the first to show that rat laminae I–II contained several morphological types of PAFs. They found that, all along its medial-to-lateral extension, lamina II$_i$, which, as shown here and in previous studies (Bailey and Ribeiro-da-Silva 2006), is the site of termination of IB4$^+$ PAFs, housed numerous finely undulating C-fibers with large *terminal boutons*. The morphology of the HRP-filled boutons detected after LM examination by Cruz and co-workers is fully compatible to that of the IB4$^+$ GIa that we have here observed at TEM. Their observations provided good support to the view that the termination of the different types/subtypes of PAFs in lamina II was not random. Other studies added additional pieces of information and led to conclude that C-fibers terminals in the superficial dorsal horn also followed a precise somatotopic pattern in rat (Molander and Grant 1985) and mouse (Odagaki et al. 2019). In specific, the lumbar segments of the spinal cord receive afferents from the hind limb, with fibers originating from the foot occupying the medial (from the digits and the plantar surface) and middle (from the medial, lateral and dorsal surfaces of the foot) third of the dorsal horn. Thus, the DT-induced disappearance of IB4$^+$/GINIP$^+$ GIa in the medial half of lamina II provides a strong histological substrate to confirm the intervention of GINIP-expressing neurons in the modulation of chemical pain after intraplantar-injected formalin (Urien et al. 2017).

Non-peptidergic IB4$^+$ C-Ncs Expressing TRPV1

The second group of murine C-Ncs was IB4$^+$/TRPV1$^+$ but did not express GINIP.

For several reasons, TRPV1, which as here and previously demonstrated (Zwick et al. 2002; Woodbury et al. 2004; Breese et al. 2005; Bencivinni et al. 2011) was detected in a subpopulation of IB4-binding non-peptidergic C-Ncs, is of relevance to this discussion. The receptor, in fact, contributes to the elaboration of nociceptive thermal and chemical stimuli (Tominaga et al. 1998; Imamachi et al. 2009; Han et al. 2013) in physiological (Caterina et al. 1997), inflammatory (Caterina et al. 2000) and neuropathic conditions (Hudson et al. 2001). We here calculated that non-peptidergic IB4$^+$/TRPV1$^+$ were about 7% of the total of the IB4$^+$ cells, thus more numerous than previously reported by others (Zwick et al. 2002; Woodbury et al. 2004; Breese et al. 2005). Notably, these neurons did not contain GINIP, as they survived DT treatment in GINIP-DT mice, and their central projections were localized in the lateral part of lamina II$_i$.

In keeping with earlier observations in rat (Molander and Grant 1985), Odagaki et al. (2019) have very recently shown that cutaneous injections in the sacral region of the mouse pelvis resulted in the labeling of the more laterally located PAFs in the dorsal horn. Aside from technical differences, both studies converge to demonstrate that the lateral lamina II receives cutaneous afferents from the sacral dorsum irrespective that these afferents are of the C and/or Aδ type(s) in relation to the type of tracer employed (Shehab and Hughes 2011). Interestingly, Breese et al. (2005) have shown that murine IB4$^+$/TRPV1$^+$ neurons increase in number after peripheral inflammation, and very recently, these non-peptidergic C-Ncs resulted to be essential for mechanical inflammatory hypersensitivity in mice (Pinto et al. 2019). From our experiments, it appears that these neurons have a very specific territory of distribution, which is consistent with a role in tactile sensation, but the reason of such a topographic specificity remains, at present, obscure.

C-LTMRs

C-LTMRs, the third group of murine C-fibers that we have described here, are a small non-peptidergic population of PAFs only found in hairy skin (Li et al. 2011; Abraira and Ginty 2013) and principally involved in tactile sensation (Olausson et al. 2002; Seal et al. 2009; Delfini et al. 2013).

We here showed the coexistence of GINIP, VGLUT3 and TAFA4 in C-LTMRs, being the two latter molecules specifically expressed in mouse C-LTMRs (Seal et al. 2009; Li et al. 2011; Delfini et al. 2013; Gaillard et al. 2014; Reynders et al. 2015; Liu et al. 2016; Urien et al. 2017). We also observed that the non-peptidergic TAFA4$^+$/VGLUT3$^+$ C-LTMRs were about one-fourth of the total of the non-peptidergic C-Ncs, as defined after IB4 labeling. Then, having shown a near 100% coexistence of TAFA4, VGLUT3 and GINIP in individual DRG neurons, we have also noticed that the GINIP$^+$/VGLUT3$^+$ GIa made by these fibers in lamina II_{iv} disappeared after DT administration in both the medial and lateral halves of this sublamina. It is worth recalling that C-LTMRs were proposed to tonically inhibit a population of yet uncharacterized excitatory interneurons triggering the response to chemical pain in the superficial dorsal horn (Urien et al. 2017).

Ultrastructural Organization of Unmyelinated C-LTMRs

Numerous ultrastructural studies agree that the terminals of the IB4$^+$ fibers in the spinal cord dorsal horn constitute the central boutons of GIa, both in basal conditions (Bencivinni et al. 2011; Salio et al. 2014; Kambrun et al. 2018) and after peripheral nerve injury (Bailey and Ribeiro-da-Silva 2006). Ultrastructural observations are thus important to confirm function, as the non-peptidergic C-fibers specifically intervene in the composition of GIa (Ribeiro-da-Silva 2015).

Two papers up to now described the ultrastructural characteristics of the glomeruli made by C-LTMRs, with strikingly different results. Some of us (Kambrun et al. 2018) reported that the murine non-peptidergic TAFA4$^+$/VGLUT3$^+$ C-LTMRs exclusively formed GIa, whereas Larsson and Broman (2019) indicated that VGLUT3$^+$ C-LTMRs were the central terminals of GII in lamina II_i of both mouse and rat.

The observation that C-LTMRs display a specific GIa glomerular configuration was not surprising if one takes into consideration their slow conduction velocities (Li et al. 2011; Abraira and Ginty 2013; Olson et al. 2016) and lack of neuropeptides (Seal et al. 2009; Li et al. 2011; Lou et al. 2013; Reynders et al. 2015; Urien et al. 2017). In addition, we here observed that TAFA4 immunoreactivity was specifically localized to lamina II_{iv} in agreement with previous studies showing that C-LTMRs terminated in lamina II_i (Li et al. 2011; Abraira and Ginty 2013; Abraira et al. 2017). Then, the notion that *bona fide* C-LTMRs only give rise to GIa in lamina II obtains strong support by the observation of the complete disappearance of these glomeruli in DT-treated *ginip* conditional mice.

The results of Larsson and Broman (2019) are difficult to explain, as the *central boutons* of GIIa are made by Aδ LTMRs and those of GIIb by Aβ fibers (Ribeiro-Da-Silva and De Koninck 2008). Larsson and Broman have identified C-LTMRs only on immunoreactivity for VGLUT3, a marker that might not be exclusive for this type of fibers (see below), whereas we have confirmed the functional type of C-LTMRs also after TAFA4 and GINIP immunostaining. Larsson and Broman carefully used three different antibodies against VGLUT3 in their study, one of which was previously tested by others in VGLUT3 KO mice (Stensrud et al. 2013). Thus, antibody specificity should not have been an issue in their material. Hoverer, validation of the VGLUT3 antibody was carried out only in very young animals and Stensrud et al. have reported coexistence of VGLUT3 with vesicular GABA transporter (VGAT), a type of association never observed in spinal cord, as VGAT has never been localized in PAFs (Merighi 2018).

There may be several other technical reasons to explain the differences in the outcomes of these few studies on the ultrastructure of C-LTMRs, but further observations will be undoubtedly necessary to clarify this issue. One interesting additional development would be to stain for these fibers in VGLUT3 knockout mice and check for disappearance of GII in the substantia gelatinosa. Indeed, Peirs et al. (2015) have demonstrated, at light level, the lack of VGLUT3 in C-LTMRs from KO mice. However, they also showed that, under allodynic conditions, expression of the transporter occurred transiently (P5-P20) in deep dorsal horn neurons.

Therefore, the pattern of expression of the transporter appears to be more complex than at first hypothesized. The issue is further complicated by the observation that in adult rats VGLUT3 was upregulated in lumbar laminae I–II in response to a visceral inflammatory stimulus (Yang et al. 2012). Thus, additional light and ultrastructural studies on the developmental expression of the transporter, regulation of its expression under increased nociceptive conditions, and a careful comparison of data obtained in normal and transgenic mice will be essential to clarify in full the pattern of expression of VGLUT3 in synaptic glomeruli.

In conclusion, we here have shown the existence of three different subpopulations of murine C-type DRG neurons: the $IB4^+/GINIP^+/TRPV1^-$ C-Ncs, the $IB4^+/GINIP^-/TRPV1^+$ C-Ncs and the C-LTMRs expressing VGLUT3, TAFA4, and GINIP. We also described the pattern of distribution of the central projections of these neurons in spinal cord lamina II at the light and electron microscopic levels, as well as the effects of GINIP ablation in conditional KO mice. Our observations provided a more in-depth characterization of the neurochemistry of these three populations of neurons in the adult mouse. With the limitations chiefly related to the differences in the distribution of TRPV1 in rat and humans, we hope that they will be useful to fuel other studies aiming to a better comprehension of the functional role of C-type DRG neurons across species, particularly in the processing of normal and pathologic pain.

Acknowledgements This work was supported by a grant from Compagnia San Paolo (Fondi di Ateneo 2012) to CS.

Author Contributions CS, AMo and AM conceived the project; PA and CS performed LM and EM experiments; CS performed the statistical analysis; AMo and PM generated the TAFA4 knock-in mouse model and the GINIP mouse model. CS and AM wrote the paper.

Compliance with Ethical Standards

Conflict of interest The authors declare that they have no conflict of interest.

Ethical Approval All procedures performed in studies involving animals were in accordance with the ethical standards of the institution or practice at the University of Turin.

References

Abraira VE, Ginty DD (2013) The sensory neurons of touch. Neuron 79:618–639. https://doi.org/10.1016/j.neuron.2013.07.051

Abraira VE, Kuehn ED, Chirila AM, Springel MW, Toliver AA, Zimmerman AL, Orefice LL, Boyle KA, Bai L, Song BJ, Bashista KA, O'Neill TG, Zhuo J, Tsan C, Hoynoski J, Rutlin M, Kus L, Niederkofler V, Watanabe M, Dymecki SM, Nelson SB, Heintz N, Hughes DI, Ginty DD (2017) The cellular and synaptic architecture of the mechanosensory dorsal horn. Cell 168(1–2):295–310. https://doi.org/10.1016/j.cell.2016.12.010

Bailey AL, Ribeiro-da-Silva A (2006) Transient loss of terminals from non-peptidergic nociceptive fibers in the substantia gelatinosa of spinal cord following chronic constriction injury of the sciatic nerve. Neuroscience 138:675–690. https://doi.org/10.1016/j.neuroscience.2005.11.051

Bencivinni I, Ferrini F, Salio C, Beltramo M, Merighi A (2011) The somatostatin analogue octreotide inhibits capsaicin-mediated activation of nociceptive primary afferent fibres in spinal cord lamina II (substantia gelatinosa). Eur J Pain 15:591–599. https://doi.org/10.1016/j.ejpain.2010.11.001

Braz JM, Nassar MA, Wood JN, Basbaum AI (2005) Parallel "pain" pathways arise from subpopulations of primary afferent nociceptor. Neuron 47:787–793. https://doi.org/10.1016/j.neuron.2005.08.015

Breese NM, George AC, Pauers LE, Stucky CL (2005) Peripheral inflammation selectively increases TRPV1 function in IB4-positive sensory neurons from adult mouse. Pain 115:37–49. https://doi.org/10.1016/j.pain.2005.02.010

Calorio C, Gavello D, Gurina L, Salio C, Sassoè-Pognetto M, Riganti C, Bianchi FT, Hofer NT, Tuluc P, Obermair GJ, Defilippi P, Balzac F, Turco E, Bett GC, Rasmusson RL, Carbone E (2019) Impaired chromaffin cell excitability and exocytosis in autistic Timothy syndrome TS2-neo mouse rescued by L-type calcium channel blockers. J Physiol 597:1705–1733. https://doi.org/10.1113/JP277487

Caterina MJ, Schumacher MA, Tominaga M, Rosen TA, Levine JD, Julius D (1997) The capsaicin receptor: a heat-activated ion channel in the pain pathway. Nature 389:816–824. https://doi.org/10.1038/39807

Caterina MJ, Leffler A, Malmberg AB, Martin WJ, Trafton J, Petersen-Zeitz KR, Koltzenburg M, Basbaum AI, Julius D (2000) Impaired nociception and pain sensation in mice lacking the capsaicin receptor. Science 288:306–313. https://doi.org/10.1126/science.288.5464.306

Cavanaugh DJ, Chesler AT, Bráz JM, Shah NM, Julius D, Basbaum AI (2011) Restriction of transient receptor potential vanilloid-1 to the peptidergic subset of primary afferent neurons follows its developmental downregulation in nonpeptidergic neurons. J Neurosci 31:10119–10127. https://doi.org/10.1523/JNEUROSCI.1299-11.2011

Cavanaugh DJ, Lee H, Lo L, Shields SD, Zylka MJ, Basbaum AI, Anderson DJ (2009) Distinct subsets of unmyelinated primary sensory fibers mediate behavioral responses to noxious thermal and mechanical stimuli. Proc Natl Acad Sci USA 106:9075–9080. https://doi.org/10.1073/pnas.0901507106

Ciglieri E, Ferrini F, Boggio E, Salio C (2016) An improved method for in vitro morphofunctional analysis of mouse dorsal root ganglia. Ann Anat 207:62–67. https://doi.org/10.1016/j.aanat.2016.04.032

Cruz F, Lima D, Coimbra A (1987) Several morphological types of terminal arborizations of primary afferents in laminae I-II of the rat spinal cord, as shown after HRP labeling and Golgi impregnation. J Comp Neurol 261:221–236. https://doi.org/10.1002/cne.902610205

Delfini MC, Mantilleri A, Gaillard S, Hao J, Reynders A, Malapert P, Alonso S, François A, Barrere C, Seal R, Landry M, Eschallier A, Alloui A, Bourinet E, Delmas P, Le Feuvre Y, Moqrich A (2013) TAFA4, a chemokine-like protein, modulates injury-induced mechanical and chemical pain hypersensitivity in mice. Cell Rep 5:378–388. https://doi.org/10.1016/j.celrep.2013.09.013

Gaillard S, Lo Re L, Mantilleri A, Hepp R, Urien L, Malapert P, Alonso S, Deage M, Kambrun C, Landry M, Low SA, Alloui A, Lambolez B, Scherrer G, Le Feuvre Y, Bourinet E, Moqrich A (2014) GINIP, a Gai-interacting protein, functions as a key

modulator of peripheral GABAB receptor-mediated analgesia. Neuron 84:123–136. https://doi.org/10.1016/j.neuron.2014.08.056

Gibson SJ, Polak JM, Bloom SR, Sabate IM, Mulderry PM, Ghatei MA, McGregor GP, Morrison JF, Kelly JS, Evans RM (1984) Calcitonin gene-related peptide immunoreactivity in the spinal cord of man and of eight other species. J Neurosci 4(12):3101–3111. https://doi.org/10.1523/JNEUROSCI.04-12-03101.1984

Guo A, Vulchanova L, Wang J, Li X, Elde R (1999) Immunocytochemical localization of the vanilloid receptor 1 (VR1): relationship to neuropeptides, the P2X3 purinoceptor and IB4 binding sites. Eur J Neurosci 11:946–958. https://doi.org/10.1046/j.1460-9568.1999.00503.x

Haberberger RV, Barry C, Dominguez N, Matusica D (2019) Human dorsal root ganglia. Front Cell Neurosci 13:271–287. https://doi.org/10.3389/fncel.2019.00271

Han L, Ma C, Liu Q, Weng HJ, Cui Y, Tang Z, Kim Y, Nie H, Qu L, Patel KN, Li Z, McNeil B, He S, Guan Y, Xiao B, Lamotte RH, Dong X (2013) A subpopulation of nociceptors specifically linked to itch. Nat Neurosci 16:174–182. https://doi.org/10.1038/nn.3289

Hsieh YL, Lin CL, Chiang H, Fu YS, Lue JH, Hsieh ST (2012) Role of peptidergic nerve terminals in the skin: reversal of thermal sensation by calcitonin gene-related peptide in TRPV1-depleted neuropathy. PLoS ONE 7:e50805. https://doi.org/10.1371/journal.pone.0050805

Hudson LJ, Bevan S, Wotherspoon G, Gentry C, Fox A, Winter J (2001) VR1 protein expression increases in undamaged DRG neurons after partial nerve injury. Eur J Neurosci 13:2105–2114. https://doi.org/10.1046/j.0953-816x.2001.01591.x

Hwang SJ, Oh JM, Valtschanoff JG (2005) Expression of the vanilloid receptor TRPV1 in rat dorsal root ganglion neurons supports different roles of the receptor in visceral and cutaneous afferents. Brain Res 1047:261–266. https://doi.org/10.1016/j.brainres.2005.04.036

Imamachi N, Park GH, Lee H, Anderson DJ, Simon MI, Basbaum AI, Han SK (2009) TRPV1-expressing primary afferents generate behavioral responses to pruritogens via multiple mechanisms. Proc Natl Acad Sci USA 106(27):11330–11335. https://doi.org/10.1073/pnas.0905605106

Kambrun C, Roca-Lapirot O, Salio C, Landry M, Moqrich A, Le Feuvre Y (2018) TAFA4 reverses mechanical allodynia through activation of GABAergic transmission and microglial process retraction. Cell Rep 22:2886–2897. https://doi.org/10.1016/j.celrep.2018.02.068

Larsson M, Broman J (2019) Synaptic organization of VGLUT3 expressing low-threshold mechanosensitive C fiber terminals in the rodent spinal cord. eNeuro. https://doi.org/10.1523/ENEURO.0007-19.2019

Lawson SN, McCarthy PW, Prabhakar E (1996) Electrophysiological properties of neurons with CGRP-like immunoreactivity in rat dorsal root ganglia. J Comp Neurol 365:355–366. https://doi.org/10.1002/(SICI)1096-9861(19960212)365:3%3c355:AID-CNE2%3e3.0.CO;2-3

Lawson SN, Perry MJ, Prabhakar E, McCarthy PW (1993) Primary sensory neurons: neurofilament, neuropeptides, and conduction velocity. Brain Res Bull 30:239–243. https://doi.org/10.1016/0361-9230(93)90250-F

Lawson JJ, McIlwrath SL, Woodbury CJ, Davis BM, Koerber HR (2008) TRPV1 unlike TRPV2 is restricted to a subset of mechanically insensitive cutaneous nociceptors responding to heat. J Pain 9(4):298–308. https://doi.org/10.1016/j.jpain.2007.12.001

Le Pichon CE, Chesler AT (2014) The functional and anatomical dissection of somatosensory subpopulations using mouse genetics. Front Neuroanat 8:21–38. https://doi.org/10.3389/fnana.2014.00021

Li L, Rutlin M, Abraira VE, Cassidy C, Kus L, Gong S, Jankowski MP, Luo W, Heintz N, Koerber HR, Woodbury CJ, Ginty DD (2011) The functional organization of cutaneous low-threshold mechanosensory neurons. Cell 147:1615–1627. https://doi.org/10.1016/j.cell.2011.11.027

Liu Z, Wang F, Fischer G, Hogan QH, Yu H (2016) Peripheral nerve injury induces loss of nociceptive neuron-specific Gαi-interacting protein in neuropathic pain rat. Mol Pain 12:1–10. https://doi.org/10.1177/1744806916646380

Lopes DM, Malek N, Edye M, Jager SB, McMurray S, McMahon SB, Denk F (2017) Sex differences in peripheral not central immune responses to pain-inducing injury. Sci Rep 7:16460. https://doi.org/10.1038/s41598-017-16664-z

Lou S, Duan B, Vong L, Lowell BB, Ma Q (2013) Runx1 controls terminal morphology and mechanosensitivity of VGLUT3-expressing C-mechanoreceptors. J Neurosci 33:870–882. https://doi.org/10.1523/JNEUROSCI.3942-12.2013

Luby-Phelps K, Ning G, Fogerty J, Besharse JC (2003) Visualization of identified GFP-expressing cells by light and electron microscopy. J Histochem Cytochem 51:271–274. https://doi.org/10.1177/002215540305100301

Merighi A (2018) The histology, physiology, neurochemistry and circuitry of the substantia gelatinosa Rolandi (lamina II) in mammalian spinal cord. Prog Neurobiol 169:91–134. https://doi.org/10.1016/j.pneurobio.2018.06.012

Merighi A, Polak JM (1993) Postembedding immunogold staining. In: Cuello A (ed) Immunohistochemistry II. Wiley, London, pp 229–264

Michael GJ, Priestley JV (1999) Differential expression of the mRNA for the vanilloid receptor subtype 1 in cells of the adult rat dorsal root and nodose ganglia and its downregulation by axotomy. J Neurosci 19:1844–1854. https://doi.org/10.1523/JNEUROSCI.19-05-01844.1999

Molander C, Grant G (1985) Cutaneous projections from the rat hindlimb foot to the substantia gelatinosa of the spinal cord studied by transganglionic transport of WGA-HRP conjugate. J Comp Neurol 237:476–484. https://doi.org/10.1002/cne.902370405

National Research Council (US) Committee on Guidelines for the Use of Animals in Neuroscience and Behavioral Research (2003) Guidelines for the Care and Use of Mammals in Neuroscience and Behavioral Research (2003) Washington (DC): National Academies Press (US); B, Estimating Animal Numbers. https://www.ncbi.nlm.nih.gov/books/NBK43325/

Odagaki K, Kameda H, Hayashi T, Sakurai M (2019) Mediolateral and dorsoventral projection patterns of cutaneous afferents within transverse planes of the mouse spinal dorsal horn. J Comp Neurol 527:972–984. https://doi.org/10.1002/cne.24593

Olausson H, Lamarre Y, Backlund H, Morin C, Wallin BG, Starck G, Ekholm S, Strigo I, Worsley K, Vallbo AB, Bushnell MC (2002) Unmyelinated tactile afferents signal touch and project to insular cortex. Nat Neurosci 5:900–904. https://doi.org/10.1038/nn896

Olson W, Dong P, Fleming M, Luo W (2016) The specification and wiring of mammalian cutaneous low-threshold mechanoreceptors. Wiley Interdisc Rev Dev Biol 5:389–404. https://doi.org/10.1002/wdev.229

Patil MJ, Hovhannisyan AH, Akopian AN (2018) Characteristics of sensory neuronal groups in CGRP-cre-ER reporter mice: comparison to Nav1.8-cre, TRPV1-cre and TRPV1-GFP mouse lines. PLoS ONE 13:e0198601. https://doi.org/10.1371/journal.pone.0198601

Peirs C, Williams S-PG, Zhao X, Walsh CE, Gedeon JY, Cagle NE, Goldring AC, Hioki H, Liu Z, Marell PS, Seal RP (2015) Dorsal horn circuits for persistent mechanical pain. Neuron 87:797–812. https://doi.org/10.1016/j.neuron.2015.07.029

Pinto LG, Souza GR, Kusuda R, Lopes AH, Sant'Anna MB, Cunha FQ, Ferreira SH, Cunha TM (2019) Non-peptidergic nociceptive neurons are essential for mechanical inflammatory hypersensitivity

in mice. Mol Neurobiol 56:5715–5728. https://doi.org/10.1007/s12035-019-1494-5

Pitcher M, Le Pichon CL, Chesler A (2016) Functional properties of C-low threshold mechanoreceptors (C-LTMRs) in nonhuman mammals. In: Olausson H, Wessberg J, Morrison I, McGlone F (eds) Affective touch and the neurophysiology of CT afferents. Springer Science+Business Media, New York, pp 31–48

Price TJ, Flores CM (2007) Critical evaluation of the colocalization between calcitonin gene-related peptide, substance P, transient receptor potential vanilloid subfamily type 1 immunoreactivities, and isolectin B4 binding in primary afferent neurons of the rat and mouse. J Pain 8:263–272. https://doi.org/10.1016/j.jpain.2006.09.005

Reynders A, Mantilleri A, Malapert P, Rialle S, Nidelet S, Laffray S, Beurrier C, Bourinet E, Moqrich A (2015) Transcriptional profiling of cutaneous MRGPRD free nerve endings and C-LTMRs. Cell Rep 10:1007–1019. https://doi.org/10.1016/j.celrep.2015.01.022

Ribeiro-Da-Silva A (2015) Substantia gelatinosa of the spinal cord. In: Paxinos G (ed) The rat nervous system, 4th edn. Elsevier Academic Press, San Diego, pp 97–114

Ribeiro-Da-Silva A, De Koninck Y (2008) Morphological and neurochemical organization of the spinal dorsal horn. In: Albright TD, Masland RH, Dallos P, Oertel D, Firestein S, Beauchamp GK, Bushnell MC, Basbaum AI, Kaas JH, Gardner EP (eds) The senses: a comprehensive reference. Academic Press, New York, pp 279–310

Ruscheweyh R, Forsthuber L, Schoffnegger D, Sandkühler J (2007) Modification of classical neurochemical markers in identified primary afferent neurons with Abeta-, Adelta-, and C-fibers after chronic constriction injury in mice. J Comp Neurol 502:325–336. https://doi.org/10.1002/cne.21311

Salio C, Lossi L, Merighi A (2011) Combined light and electron microscopic visualization of neuropeptides and their receptors in central neurons. Methods Mol Biol 789:57–71. https://doi.org/10.1007/978-1-61779-310-3_3

Salio C, Lossi L, Ferrini F, Merighi A (2005) Ultrastructural evidence for a pre- and postsynaptic localization of full-length trkB receptors in substantia gelatinosa (lamina II) of rat and mouse spinal cord. Eur J Neurosci 22:1951–1966. https://doi.org/10.1111/j.1460-9568.2005.04392.x

Salio C, Ferrini F, Muthuraju S, Merighi A (2014) Presynaptic modulation of spinal nociceptive transmission by glial cell line-derived neurotrophic factor (GDNF). J Neurosci 34:13819–13833. https://doi.org/10.1523/JNEUROSCI.0808-14

Seal RP, Wang X, Guan Y, Raja SN, Woodbury CJ, Basbaum AI, Edwards RH (2009) Injury-induced mechanical hypersensitivity requires C low threshold mechanoreceptors. Nature 462:651–655. https://doi.org/10.1038/nature08505

Shehab SA, Hughes DI (2011) Simultaneous identification of unmyelinated and myelinated primary somatic afferents by co-injection of isolectin B4 and cholera toxin subunit B into the sciatic nerve of the rat. J Neurosci Methods 198:213–221. https://doi.org/10.1016/j.jneumeth.2011.04.002

Silverman JD, Kruger L (1990) Selective neuronal glycoconjugate expression in sensory and autonomic ganglia: relation of lectin reactivity to peptide and enzyme markers. J Neurocytol 19:789–801. https://doi.org/10.1007/bf01188046

Stensrud MJ, Chaudhry FA, Leergaard TB, Bjaalie JG, Gundersen V (2013) Vesicular glutamate transporter-3 in the rodent brain: vesicular colocalization with vesicular γ-aminobutyric acid transporter. J Comp Neurol 521:3042–3056. https://doi.org/10.1002/cne.23331

Stephens KE, Zhou W, Ji Z, Chen Z, He S, Ji H, Guan Y, Taverna SD (2019) Sex differences in gene regulation in the dorsal root ganglion after nerve injury. BMC Genomics 20:147–165. https://doi.org/10.1186/s12864-019-5512-9

Stucky CL, Lewin GR (1999) Isolectin B(4)-positive and-negative nociceptors are functionally distinct. J Neurosci 19:6497–6505. https://doi.org/10.1523/JNEUROSCI.19-15-06497.1999

Tominaga M, Caterina MJ, Malmberg AB, Rosen TA, Gilbert H, Skinner K, Raumann BE, Basbaum AI, Julius D (1998) The cloned capsaicin receptor integrates multiple pain-producing stimuli. Neuron 21(3):531–543. https://doi.org/10.1016/S0896-6273(00)80564-4

Urien L, Gaillard S, Lo Re L, Malapert P, Bohic M, Reynders A, Moqrich A (2017) Genetic ablation of GINIP-expressing primary sensory neurons strongly impairs Formalin-evoked pain. Sci Rep 7:43493. https://doi.org/10.1038/srep43493

Usoskin D, Furlan A, Islam S, Abdo H, Lönnerberg P, Lou D, Hjerling-Leffler J, Haeggström J, Kharchenko O, Kharchenko PV, Linnarsson S, Ernfors P (2015) Unbiased classification of sensory neuron types by large-scale single-cell RNA sequencing. Nat Neurosci 18(1):145–153. https://doi.org/10.1038/nn.3881

Vrontou S, Wong AM, Rau KK, Koerber HR, Anderson DJ (2013) Genetic identification of C fibres that detect massage-like stroking of hairy skin in vivo. Nature 493(7434):669–673. https://doi.org/10.1038/nature11810

Zheng Y, Liu P, Bai L, Trimmer JS, Bean BP, Ginty DD (2019) Deep sequencing of somatosensory neurons reveals molecular determinants of intrinsic physiological properties. Neuron 103(4):598–616.e7. https://doi.org/10.1016/j.neuron.2019.05.039

Zwick M, Davis BM, Woodbury CJ, Burkett JN, Koerber HR, Simpson JF, Albers KM (2002) Glial cell line-derived neurotrophic factor is a survival factor for isolectin B4-positive, but not vanilloid receptor 1-positive, neurons in the mouse. J Neurosci 22(10):4057–4065. https://doi.org/10.1523/JNEUROSCI.22-10-04057.2002

Wang BL, Larsson LI (1985) Simultaneous demonstration of multiple antigens by indirect IMF or immunogold staining. Novel light and electron microscopical double and triple staining method employing primary antibodies from the same species. Histochemistry 83:47–56. https://doi.org/10.1007/bf00495299

Woodbury CJ, Zwick M, Wang S, Lawson JJ, Caterina MJ, Koltzenburg M, Albers KM, Koerber HR, Davis BM (2004) Nociceptors lacking TRPV1 and TRPV2 have normal heat responses. J Neurosci 24(28):6410–6415. https://doi.org/10.1523/JNEUROSCI.1421-04.2004

Yang CQ, Wei YY, Leng YX, Zhong CJ, Zhang YS, Wan Y, Duan LP (2012) Vesicular glutamate transporter-3 contributes to visceral hyperalgesia induced by *Trichinella spiralis* infection in rats. Dig Dis Sci 57:865–872. https://doi.org/10.1007/s10620-011-1970-x